STRENGTH TESTING OF IN-SERVICE ASPHALT PAVEMENTS

IN MANITOBA AND CORRELATION TO RUTTING

Myron Thiessen, Graduate Student
Dept. of Civil Engineering, University of Manitoba
Winnipeg, Manitoba

Ahmed Shalaby, Assistant Professor
Dept. of Civil Engineering, University of Manitoba
Winnipeg, Manitoba

Leonnie Kavanagh, Surfacing Materials Engineer
Materials and Research Branch,
Manitoba Highways and Government Services
Winnipeg, Manitoba

ACKNOWLEDGEMENTS

The funding received from the Natural Sciences and Engineering Research Council and Manitoba Department of Highways and Government Services is gratefully acknowledged. The authors wish to thank Mr. B. Parobec, Material and Research Laboratory, Manitoba Highways, and Mr. K. Lynch, Civil Engineering Laboratories, University of Manitoba for supporting the laboratory testing.

ABSTRACT

This research investigates strength and rutting performance of in-service asphalt pavements in Manitoba using a form of the indirect tensile strength test. Existing methods to evaluate the strength of hot mix asphalt pavements have relied primarily on past experience as well as mix volumetric, stability and flow properties. The application of strength-based test methods is a significant shift from these practices.

Cored samples were collected from seven sections across the province representing a spectrum of traffic and climatic conditions. Two groups of asphalt concrete cores were extracted from each section: one group from the wheel paths and a second group from the areas between wheel paths. Three sampling areas were randomly selected along each section, and in total 21 cores from each paving project were retrieved. Mix volumetric properties were determined from 12 of the core samples while two samples per site were tested for strength and deformation using a form of the indirect tensile strength test at 25°C. The specimens were loaded diametrally at a slow loading rate and the horizontal and vertical deformations were measured on-sample according to ASTM D 4123. Correlations between strength, deformations, rutting, and mix volumetric properties were determined and presented.

RÉSUMÉ

Cette recherche examine, au moyen d'un type d'essai de traction indirecte, la résistance et la performance à l'orniérage des revêtements bitumineux en service au Manitoba. Les méthodes existantes pour évaluer la résistance des revêtements d'enrobés bitumineux à chaud ont compté sur l'expérience passée ainsi que sur la volumétrie, la stabilité et les propriétés de déformation des enrobés. L'application des méthodes d'essais basées sur la résistance est un changement important de ces pratiques.

Des carottes ont été prélevées sur sept sections à travers la province représentant la gamme des conditions de trafic et de climat. Deux groupes de carottes de béton bitumineux ont été prélevés sur chaque section: un groupe dans les pistes de roues, et le second entre les pistes. Trois endroits d'échantillonnage ont été choisis au hasard le long de chaque section, et un total de 21 carottes sur chaque projet de pavage ont été extraites. Les propriétés volumétriques des enrobés ont été déterminées sur 12 des carottes alors qu'on a fait sur deux échantillons par site des tests de résistance et de déformation au moyen d'un type d'essai de traction indirecte à 25°C. Les échantillons ont été mis en charge diamétralement à un faible taux de chargement et les déformations horizontales et verticales ont été mesurées sur l'échantillon selon la méthode ASTM D 4123. Des corrélations entre la résistance, les déformations, l'orniérage et les propriétés volumétriques des enrobés ont été déterminées et sont présentées.

1.0 INTRODUCTION

Approximately 600,000 tonnes of virgin and recycled asphalt mix are produced and placed annually by the Manitoba Department of Highways. Due to external demands to increase axle loading and vehicle weights on the highway network, the Department of Highways is examining the performance of their pavements under these higher loadings. Therefore the Department is looking at quantitatively evaluating its bituminous mixes using a simple, low-cost laboratory test to measure their relative strength and assess their resistance to rutting.

Rutting in asphalt pavements is generally associated with two types of deformation as shown in Figure 1: (1) structural rutting caused by weak or insufficient pavement structure; and (2) permanent deformation of the asphalt concrete caused by plastic flow of the bound material under repeated load. While the structural rutting occurs primarily during spring thaw periods, plastic deformations occur under warm temperature conditions and heavy or slow-moving traffic. Rutting failure in asphalt concrete is initiated by a combination of low binder cohesion often associated with high binder content, and weak aggregate skeleton lacking stone on stone contact and aggregate interlock. The data collected in this research pertains to thick or overlaid pavements and in such case rutting is almost solely caused by the instability of the asphalt mix. This paper will investigate rutting due to plastic deformations only, and will focus primarily on the strength and volumetric properties of the asphalt concrete.

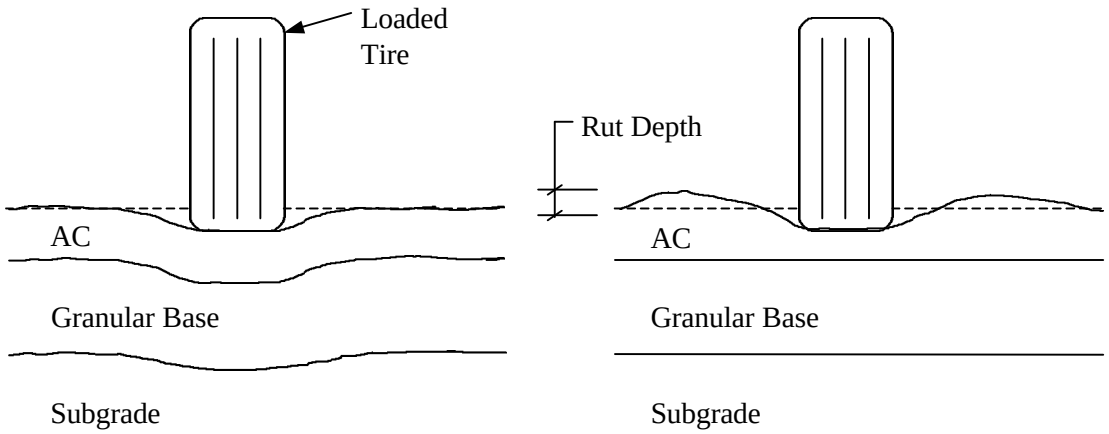

a) Structural Rutting Caused by Weak Pavement Structure

b) Rutting Caused by Plastic Flow of the Asphalt Concrete (AC) Layer

Figure 1: Types and Causes of Rutting

Cored samples were collected from seven representative highway sections across the province with varying traffic and climatic conditions. Two groups of asphalt concrete cores were extracted from each section: one group from the inside and outside wheel paths of the pavements and a second group from the areas between wheel paths. Three sampling areas were randomly selected along each section, and in total, 21 cores from each highway project were retrieved. Mix volumetric properties were determined from 12 of the core samples while two samples per site were tested for strength and performance parameters. Performance of the samples was determined using a form of the indirect tensile strength test at 25°C. The specimens were loaded diametrally at a slow loading rate and the horizontal and vertical deformations were measured on-sample as outlined in ASTM D 4123 [1].

2.0 COMPARISON OF STRENGTH TESTING PROTOCOLS

The application of laboratory test methods to evaluate the strength and fundamental material properties of asphalt concrete represents a significant shift from past mix design practice. Traditional asphalt mix design systems, such as the Marshall system, relied primarily on experience and mix volumetric parameters and Marshall stability and flow alone, to select suitable mix designs. Although the Superpave mix design system improved upon these methods, and several strength test procedures have been applied with varying degrees of success, researchers are still in the process of developing a simple test or protocol that would relate material strength to field performance [2].

2.1 Strength Test Procedures

A literature search was carried out to compare the strength-based laboratory test methods that have been used to evaluate rutting of asphalt concrete mixes. Invariably, these tests have attempted to simulate vertical and lateral stress and compatibility conditions of an asphalt pavement under temperature-controlled conditions. A comparison of the test methods is summarized in Table 1. The tests can be grouped into the following categories: (1) unconfined creep; (2) confined creep; (3) unconfined repeated compression; (4) confined repeated compression; (5) diametral compression (indirect tension); (6) repeated shear; and (7) loaded wheel simulation (wheel-tracking).

2.1.1 Unconfined Creep

The unconfined creep test has been used extensively to determine rut susceptibility of asphalt mixes [3, 4, 5, 6, 7, 8]. Normally the test is conducted at axial stress levels ranging between 100 and 207 kPa and at a temperature of 40°C.

2.1.2 Confined Creep

The use of the confined creep test to evaluate permanent deformation characteristics of asphalt concrete is well documented in the literature. Brown and Foo [8] recommend the test be conducted at 828 kPa with a confining stress of 138 kPa at a temperature of 60°C. Others, such as Monismith and Tayebali [4], performed the test at much lower axial and confining stress levels of 207 kPa and 103 kPa, respectively, and a temperature of 40°C.

2.1.3 Unconfined Repeated Compression

Suitable test procedures for the unconfined repeated compression test have been described in detail by Kim et al. [6], Brown and Gibb [9], and Bhairampally et al. [10]. Axial stress levels vary but typically do not exceed 107 kPa. The test is generally conducted at 40°C at frequencies between 0.5 and 2.0 Hz.

2.1.4 Confined Repeated Compression

The confined repeated compression test makes use of traditional triaxial test apparatus capable of imparting repeated loads on an asphalt concrete specimen. Although stress conditions vary, loading cycles typically consisted of 0.1 second load pulses followed by 0.5-second rest periods at 40°C. Details of the test have been documented elsewhere [9, 11, 12].

Table 1: Summary of Strength Test Methods for Asphalt Concrete Mixes

Test Method	Ref	Specimen Diam (mm)	Specimen Height (mm)	Applied Stresses	Loading Pattern	Test Temp (°C)
Unconfined Creep	[3]	102	203	Axial (101, 207, 483 kPa)	60 min. load	NA
	[4]	102	203	Axial (138 kPa)	60 min. load	25, 38, 60
	[5]	102	64	Axial (103 kPa)	60 min. load; 15 min. rest	25
	[6][1]	152	102	Axial (100 kPa)	60 min. load	40
	[7]	152	NA	Axial (103 kPa)	60 min. load	40
	[8]	102	102	Axial (138 kPa)	60 min. load; 15 min. rest	40
Confined Creep	[4]	102	203	Axial (207 kPa); Confining (103 kPa)	NA	25, 38, 60
	[8]	102	102	Axial (828 kPa); Confining (138 kPa)	60 min. load; 15 min. rest	60
Unconfined Repeated Compression	[6][2]	102	203	Varied	0.125 s load; 0.375 s rest; 2000 pulses	Varied
	[9]	100	NA	Axial (100 kPa)	1 s load; 0.5 Hz; 10,000 cycles	40
	[10]	100	200	Axial (105 kPa)	NA	40
Confined Repeated Compression	[9]	100	NA	Axial (230 kPa); Confining (70 kPa)	1 s load; 1 s rest; 3,600 cycles	40
	[11]	102	203	Axial (310 kPa); Confining (207 kPa)	0.1 s load; 0.5 s rest; 12,000 cycles	40
	[12]	100	200	Axial (276 kPa); Confining (207 kPa)	0.1 s load; 0.5 s rest	40
Diametral Compression (Indirect Tension)	[13]	102	NA	Static load (51 mm/min)	Up to failure	Varied
	[14]	NA	NA	Static load (51 mm/min)	Up to failure	25
	[15]	102	NA	Dynamic load (445 N)	1 Hz	50
	[16]	102	63	Dynamic load (300 N)	0.3-60 Hz	NA
Repeated Shear	[17]	150	50	Shear (70 kPa)	0.1 s load; 0.6 s rest; 5,000 cycles	Varied
	[18]	152	102	Shear (68 kPa)	0.1 s load; 0.6 s rest; 100,000 cycles	Varied
Loaded Wheel Simulation	[19]	beams or cylinders (various sizes)		445 N wheel load; 690 kPa hose pressure	8000 cycles	30-60

Notes: [1] Shell Method; [2] Ohio State Method; NA = not available

2.1.5 Diametral Compression

The diametral compression or indirect tension test (IDT) is performed by applying a static or dynamic load to cylindrical specimens along the diametral axis. Axial and lateral deformations are measured closer to the centre of the sample, ASTM D 4123 [1]. Static diametral compression has traditionally been used to determine tensile strength while the dynamic test has been used to determine elastic properties such as resilient modulus, M_R, and Poisson's ratio, ν [13, 14, 15]. Recently, the dynamic test has been used to evaluate mixture stiffness using a viscoelastic solution to interpret the test results [16].

2.1.6 Repeated Shear

The repeated shear at constant height (RSCH) has been proposed as an effective test to evaluate rutting susceptibility in asphalt mixes [17, 18] and is supported by extensive SHRP research. In this procedure, cylindrical samples are subjected to repeated shear loads of 70 kPa at temperatures that correspond to the mean 7-day maximum pavement temperature.

2.1.7 Loaded Wheel Simulation

In the category of simulation tests, a number of attempts have been made to develop a moving wheel apparatus that can accelerate the effect of loaded tires on a pavement structure. Several loaded wheel test (LWT) devices have been developed to evaluate rutting potential in asphalt mixes including the Georgia Loaded Wheel Tester (GLWT), the Hamburg Wheel Tester (HWT), and the French Wheel Tracker (FWT). Each of these devices uses a loaded wheel to test rutting in asphalt beams or cylinders.

The most recently developed simulation device is the Asphalt Pavement Analyzer (APA), which essentially is a modified version of the GLWT. The APA closely mimics field conditions by subjecting slab or cylindrical specimens to multiple wheel loadings over a pressurized hose in a controlled environmental chamber. Loading conditions can be varied, although Kandhal and Mallick [19] utilized a wheel load of 445 N and a hose pressure of 690 kPa.

2.2 Test Selection

Although considerable research related to permanent deformation in asphalt concrete has been documented, a consensus as to which laboratory test procedure is most applicable has not yet been reached. Consequently, the selection of a test to determine the strength properties of the asphalt concrete pavements in this study was based predominantly on the availability of suitable test equipment and the simplicity of the test protocol itself. Based on these parameters, the diametral compression or indirect tensile test was chosen. The general procedures for both the static (indirect tensile strength) and dynamic (resilient modulus) indirect tensile test protocols are provided in ASTM D 4123 [1] and the new LTPP P07 [20]. A modified version of the indirect tensile strength procedure was used here as given in section 4.2.3 of this paper.

3.0 DATA COLLECTION AND FIELD SAMPLING

Cores were collected from seven asphalt concrete pavements constructed between 1989 and 1998 for the analysis. The construction data and core samples were collected in order to evaluate the as-constructed versus current mix properties and their relationship to rutting and mix strength.

3.1 Site Selection

Seven asphalt concrete paving projects in Manitoba were selected for the mix evaluation and strength testing. Project selections were based on pavements with different aggregate types, pavement age, geographic location, and traffic loading in order to provide a varied cross-section for the analysis. The project locations and pertinent construction data are listed in Table 2, and graphically represented in Figure 2. The selected pavement ages ranged from 1 to 10 years of age, and are located along the TransCanada Highway (PTH 1), the Yellowhead Highway (PTH 16), and a joint portion of PTH 3 and 14 in the south-central part of the province.

3.2 Construction History

Each project was constructed using Department of Highways mix design and construction specifications, and with QC/QA performed by the Department. The pavement structures and construction type are represented in Table 2. All existing pavements were milled prior to overlay, with the milled thickness replaced plus the overlay thickness. Of the seven pavements selected, five were asphalt overlays on asphalt or concrete pavement, while the remaining pavements were new asphalt pavements on granular or asphalt stabilized base. The overlays ranged in thickness from 75 mm to 150 mm.

3.3 Traffic

Traffic loadings (20-year Design ESALs) on the Department's highway network typically range from under one million ESALs on low volume roads, to over 20 million ESALs on higher volume routes. The traffic loading is based on Equivalent Single Axle Loads (ESALs) which are calculated from Average Annual Daily Traffic (AADT) and percent truck traffic. The ESAL calculations are for the direction of travel only. The estimated traffic loading on the seven pavements, as well as the 20-year design ESALs, are shown in Table 3.

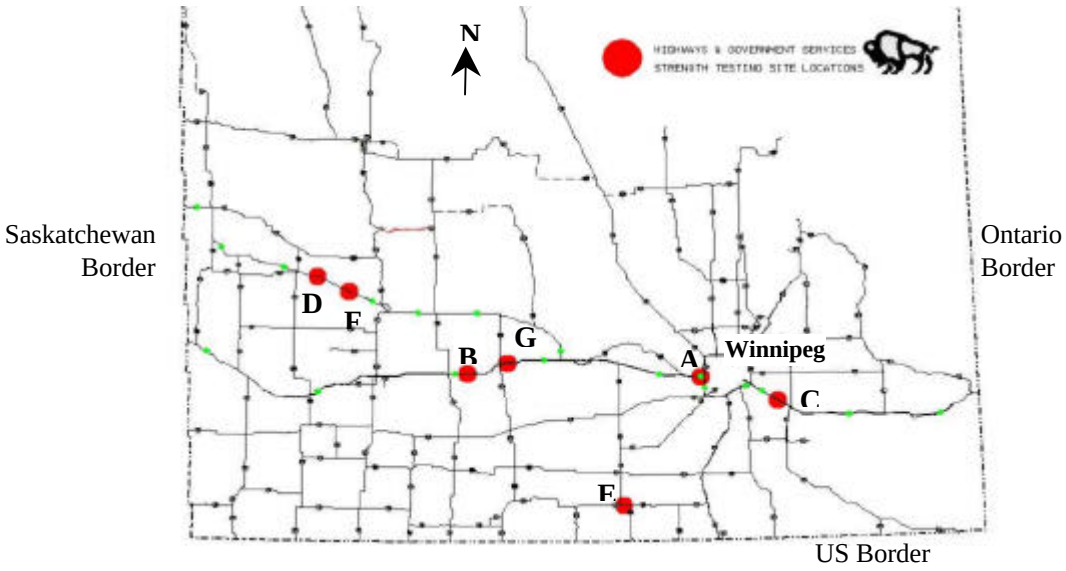

Figure 2: Project Locations

Table 2: Site Location and Construction History

Test Site	Year Built	Overlay Age	Location	Pavement Structure (Year of Construction)
A	1990	9	PTH 1, TransCanada Highway (West of Winnipeg)	75 mm asphalt overlay (1990) 75 mm asphalt (1973) 200 mm concrete (1959) 100 mm granular base (1959)
B	1989	10	PTH 1, TransCanada Highway (East of Brandon)	100 mm asphalt overlay (1989) 100 mm asphalt overlay (1977) 175 mm sand asphalt base (1977)
C	1994	5	PTH 1, TransCanada Highway (East of Winnipeg)	75 mm asphalt overlay (1994) 75 mm asphalt (1975) 203 mm concrete (1954) 152 mm granular base (1954)
D	1994	5	PTH 16, Yellowhead Highway (North of Brandon)	105 mm asphalt overlay (1994) 100 asphalt pavement (1990) 400 mm granular (1990)
E	1995	4	PTH 3 & 14 (Winkler/Morden)	100 mm asphalt overlay (1995) 125 mm stabilized base (1994) 350 mm granular sub-base (1994)
F	1996	3	PTH 16, Yellowhead Highway (North of Brandon)	150 mm asphalt (1996) 150 granular base (1995) 300 granular sub-base (1995)
G	1998	1	PTH 1, TransCanada Highway (McGregor)	85 mm asphalt overlay (1998) 35 mm asphalt pavement (1976) 203 stabilized base (1976)

Table 3: Present Traffic Data and Design Equivalent Single Axle Loads (ESALs)

Test Site	Traffic Data			20-year
	Current AADT[1]	Percent Trucks	Estimated ESALs to Date[2]	Design ESALs[3] (Year of Design)
A	8,300	12.4	8.435 M	9.0 M (1990)
B	2,860	19.4	4.982 M	3.6 M (1989)
C	7,770	9.0	3.371 M	5.3 M (1994)
D	800	24.3	1.992 M	1.2 M (1990)
E	4,020	5.9	0.795 M	3.1 M (1995)
F	800	24.3	0.724 M	2.4 M (1996)
G	2,760	20.6	0.581 M	15.7 M (1998)

Note: [1] AADT values are from 1998; per direction of travel
[2] Estimated ESALs to Date are from construction to time of testing using most recent traffic volumes and truck factors.
[3] 20-Year Design ESALs are based on expected traffic volumes and truck factors at year of construction.

3.4 As-Constructed Test Section Mix Properties

As constructed field volumetric data were collected and tabulated from the Department's historical records for each project. The as-constructed Department mix design specifications (based on 75 blow Marshall) are 4 percent Air Voids; 14-16 percent Voids in Mineral Aggregate (VMA) on wearing lift; 65-75 percent Voids Filled with Asphalt (VFA) and a stability of 3.0 kN, or greater. The as-constructed mix properties, as well as the type of asphalt cement (CGSB specification) and percent of Recycled Asphalt Product (RAP) in the mixes are identified in Table 4.

Table 4: As-Constructed Mix Properties

Test Site	Asphalt Content (%)	Core Density (kg/m^3)	Stability (kN)	In-Place Air (%)	AC Grade	Absolute Viscosity (Poise)	RAP (%)	Crush Count (1 Fractured Face) (%)
A	5.3	2382	6.1	5.1	120/150	12,237	0	NA
B	6.1	2239	7.5	7.0	120/150	8,712	0	NA
C	5.5	2262	9.4	9.3	120/150	7,851	20	53
D	6.2	2178	11.6	9.8	120/150	5,405	0	55
E	5.5	2231	16.5	8.7	150/200	6,155	23	52
F	5.9	2197	15.3	9.7	150/200	3,062	15	62
G	5.7	2273	9.5	7.3	150/200	5,414	20	60

Note: AC = asphalt cement; RAP = reclaimed asphalt pavement; NA = not available

3.5 Rut Depth Measurement

The rut depths were manually measured at the cored locations with a 1.8 metre straight edge in the inner and outer wheel paths. The rut depth measurements taken between the wheel path to the edge of lane are identified in Table 5. The rut depths range from 1.3 to 5.8 mm. Typically the Department of Highways triggers remedial action for rutting at depths over 5 mm.

Table 5: Rut Depth Measurements

Test Site	Year Built	Overlay Age	Estimated ESALs* to Date	Total Rutting in Top Lift (mm)
A	1990	9	8.435 M**	5.2
B	1989	10	4.982 M	5.8
C	1994	5	3.371 M	2.8
D	1990	9	1.992 M	3.2
E	1995	4	0.795 M	3.7
F	1996	3	0.724 M	1.3
G	1998	1	0.581 M	3.0

* ESALs = Equivalent Single Axle Loads
** M stands for million

3.6 Field Coring and Sampling

Representative 152 mm diameter cores were collected from the seven pavement structures in November 1999. The coring locations were selected at random with three sections per test site cored to obtain representative values over the entire project. Coring was performed with a Milwaukee water-cooled, diamond tooth core barrel. Each core location was tied into the Department of Highways control section referencing system for future identification. Cores were taken in the travelling lanes only in the outer wheel path, between wheel path, and inner wheel path as shown in Figure 3.

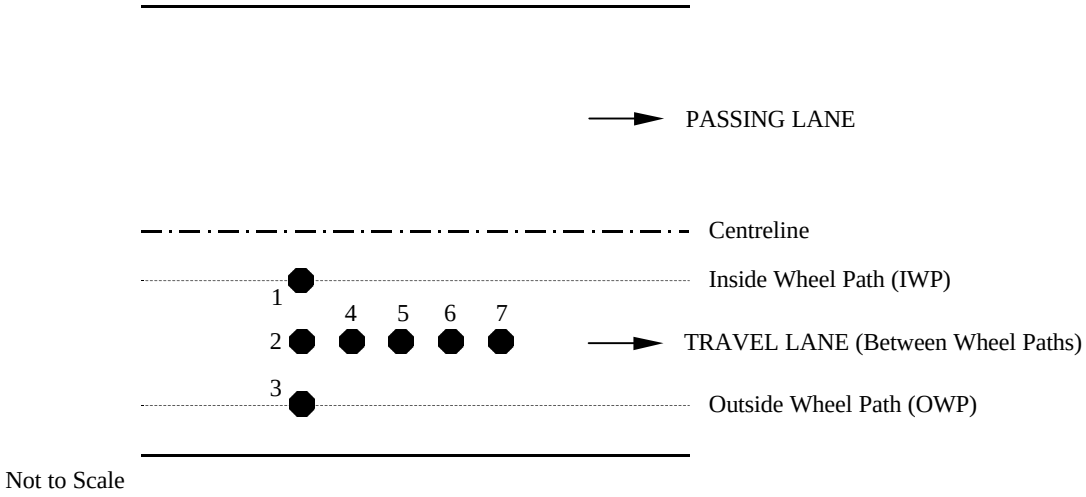

Figure 3: Core Sampling Configuration

4.0 LABORATORY AND STRENGTH TESTING PROGRAM

Laboratory testing of the core samples for volumetric properties and for strength testing was undertaken for this study. The laboratory test plan for the pavement cores is shown in Figure 4. Of the total of 21 cores taken per test site, 12 cores were identified for volumetric, binder, and aggregate analysis (cores #1-4, Figure 3), and the remaining nine for strength testing (cores #5-7, Figure 3). Of the nine cores identified for strength testing, two were randomly chosen for strength testing in this study while the remaining seven cores were retained for future testing.

4.1 Core Analysis

A series of laboratory tests were conducted on the 12 cores per project reserved for evaluation of physical mixture properties. The testing program consisted of the following tests on the top lift only to evaluate volumetric, asphalt binder, and aggregate properties:

1. Bulk density
2. In-place air voids
3. Marshall stability and flow
4. Voids analysis to measure air voids, VMA, and VFA
5. Abson method to recover the aged asphalt cement to determine asphalt content
6. Recovered binder penetration at 25°C and absolute and kinematic viscosity
7. Sieve analysis to determine the gradation of the aggregate.

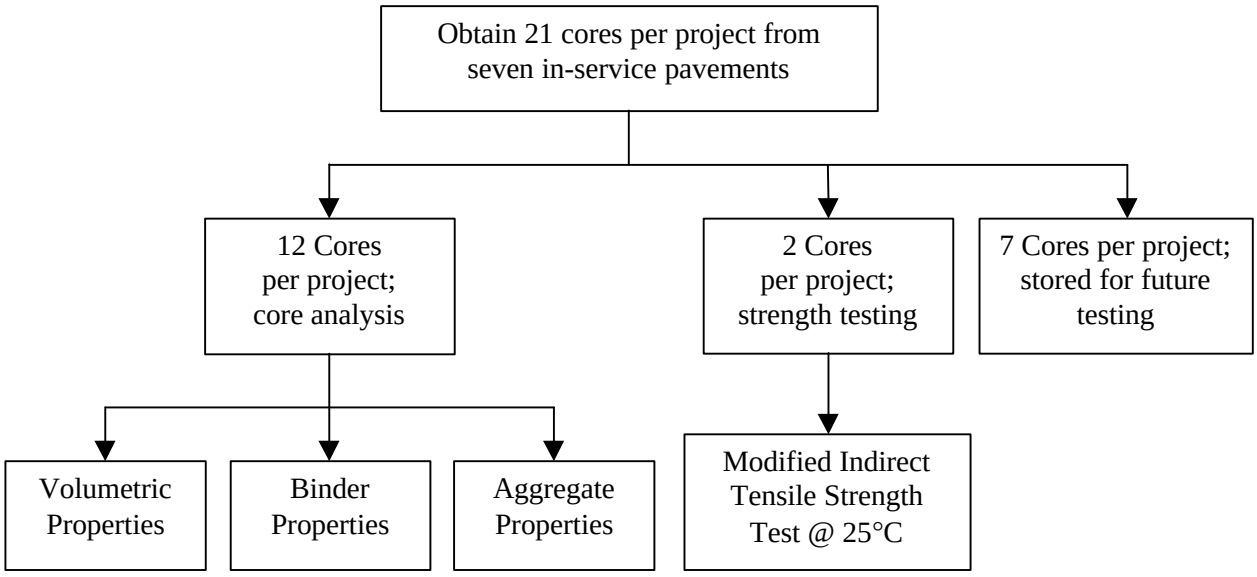

Figure 4: Laboratory Test Plan

4.2 Modified Indirect Tensile Strength Testing

4.2.1 Test Apparatus

The indirect tensile strength testing was conducted using a 100 kN stepless drive load frame, equipped with loading platens according to ASTM D 4123 [1] as shown in Figure 5. The load is transferred to the specimen via 19.4 mm wide curved loading strips with curvature equal to the diameter of the cylindrical specimens. Linear variable differential transducers (LVDTs) were placed at opposite corners of the loading platen to measure ram displacement and verify the loading rate. The entire test apparatus was placed inside a temperature-controlled room capable of maintaining temperature settings within ± 1°C. The room has a temperature range of 10 to 50°C and is large enough (approximately 1.5 m x 2.0 m) to provide adequate specimen storage during testing.

4.2.2 Sample Preparation

All cores were stored in a cold storage room until the testing program began. The two core samples selected for strength testing were sawed into lift thicknesses using a water-cooled masonry saw. The thickness and diameter of the layer samples were then measured to the nearest 0.1 mm. Sample thickness ranged from 26.2 to 43.0 mm due to variation in constructed lift heights. All samples were within acceptable thickness limits (25-50 mm) as specified in the new LTPP Protocol P07 [20]. Each cut face was inspected to ensure that a smooth surface was obtained. The cores were then instrumented with miniature LVDTs on both sides of the sample along two perpendicular axes. These were attached directly to the specimen using aluminium gauge points and epoxy glue. Two gauge points were mounted along the horizontal axis (perpendicular to loading) and another two along the vertical axis (parallel to loading). In both cases, the centre-to-centre spacing was 38.1 mm (1.5 in). Proper placement and alignment of the gauge points was ensured through the use of a standard template. All samples were placed within the temperature controlled testing chamber a minimum of 24 hours prior to testing to ensure that the samples reached the desired temperature.

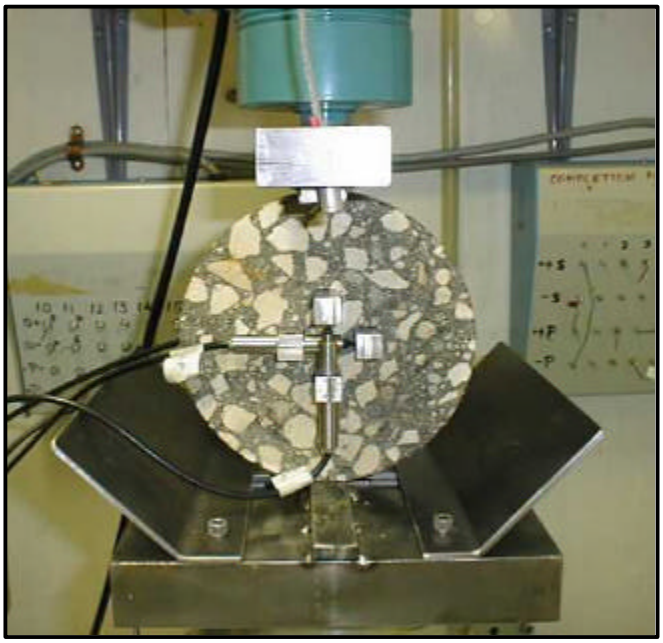

Figure 5: Test Apparatus and On-sample Instrumentation

4.2.3 Modified Indirect Tensile Strength Procedure

Specimens were tested in indirect tension using a monotonic loading rate of 0.1 mm/min. This slow loading rate was used in order to capture the load deformation response of the mixture over time and to allow plastic deformations to take place. A data acquisition system measured load and both horizontal and vertical deformations throughout the testing at a sampling rate 10 Hz. All tests were conducted at a temperature of 25°C. No preconditioning load was applied as trial testing indicated the load dissipated rapidly at this slow loading rate.

5.0 ANALYSIS OF DATA AND DISCUSSION OF RESULTS

5.1 Rutting Data

The pavement sections chosen for this study differed in age and traffic, making direct comparison of measured rut depth meaningless. It is imperative, therefore, to normalize the rut depth measurements as a function of traffic. It has been shown by Brown and Cross [21] that pavement behaviour is best modelled using a rate of rutting that is a function of the square root of total accumulated traffic, or ESALs. The rate of rutting is calculated by dividing the depth of rutting by the square root of accumulated MESALs, where MESALs is the number of ESALs in millions. For example, if the rut depth is 10 mm and the accumulated traffic is 1 million ESALs, the rate of rutting is:

$$\text{Rate of Rutting} = \frac{10\ \text{mm}}{\sqrt{1\ \text{MESALs}}} = 10\ \text{mm/MESALs}^{1/2}$$

If the same rutted pavement had accumulated 4 million ESALs of traffic, the rate of rutting would only be 5 mm/MESALs$^{1/2}$. Figure 6 compares the seven test sites according to their rate of rutting. Sites G and E

exhibit the highest rutting rates (3.94 and 4.15, respectively), although total accumulated traffic for both sites is relatively low at 581,000 and 795,000 ESALs, respectively. Conversely, sites C and F had the lowest rutting rates (1.52 and 1.53 mm/MESALs$^{1/2}$, respectively), although accumulated traffic between the two differed significantly from 3,371,000 to 724,000 ESALs. The average rate of rutting observed at all seven sites was 2.54 mm/MESALs$^{1/2}$.

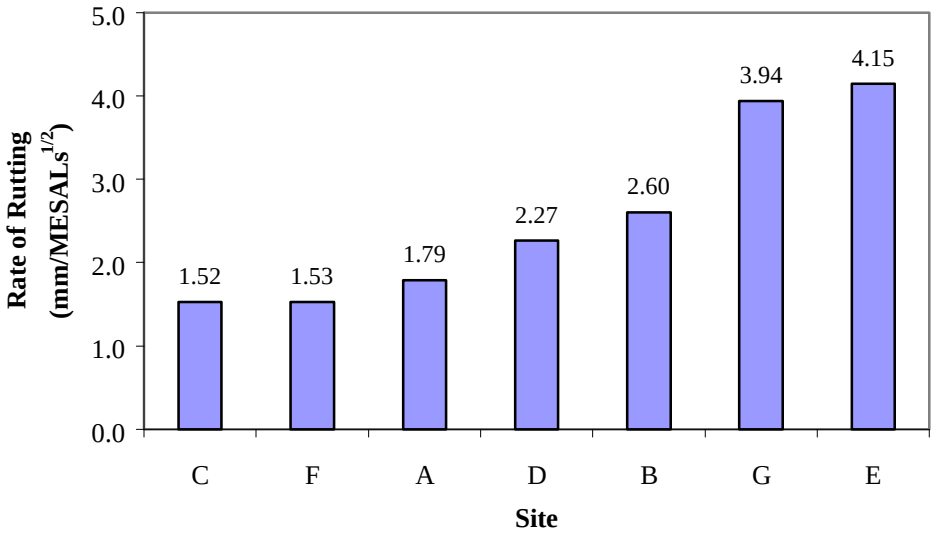

Figure 6: Rate of Rutting at Test Sites
MESALs = millions of equivalent single axles loads

5.2 Results of Core Analysis

5.2.1 Volumetric and Asphalt Binder Properties

Table 6 summarizes the volumetric and asphalt binder properties of the pavement test sites obtained from laboratory testing of the recovered cores. The results represent average values of the top lift of the 12 cores tested at each site. Average recovered asphalt content of the mixes was 6.0 percent, which is typical of asphalt surface mixtures in Manitoba. Measured air voids appear to be rather high, particularly at sites E and F, which have 5.5 and 5.9 percent air voids respectively, even after being subjected to traffic. VMA range from 13.1 to 15.3 percent, although typical mixes fall between 14 and 16 percent.

It is well documented in the literature that the material properties of an asphalt mixture have a profound effect on rutting performance. Poor performing pavements tend to have low air voids, excess asphalt content, insufficient field compaction, low binder stiffness, and poor aggregate interlock. Detailed discussion of the effect of these parameters on rutting performance is documented elsewhere [9, 14, 22, 23, 24].

A linear regression analysis was conducted to look at the relationships between the volumetric and binder properties of the cores (AC content, air voids, VMA, stability, binder penetration, and density) and rutting performance. A more elaborate analysis could not be justified at this point due to insufficient performance data. A summary of the results shown in Table 7 indicates little or no direct correlation between mix volumetric properties and rutting rate. The as-constructed values, obtained from job

summaries, and the present condition values, obtained from the analysis of recovered cores, are shown. Out of the six parameters given, only recovered binder penetration showed some correlation with an R^2 of 0.241. A plot of recovered binder penetration versus rate of rutting is shown in Figure 7. As expected, higher penetration grades tend to produce softer mixes that are more susceptible to rutting in the field. The correlation may be relatively weak because the binder contributes approximately 20 percent to rut resistance, while the remaining 80 percent is dominated by the aggregate structure. Rutting is a complex phenomenon that cannot be described by a single parameter. Rather, it is usually a number of different factors in combination that contribute to the overall rate and magnitude of rutting. This outcome underlines the importance of directly measuring mix strength and deformation parameters via a simple strength test and relating the results to field performance.

Table 6: Physical Mixture Properties of Recovered Cores

Test Site	AC (%)	Air Voids (%)	VMA (%)	VFA (%)	Stability (kN)	Flow (0.25 mm)	Density (kg/m^3)	Recovered Penetration
A	5.6	4.3	13.6	68.3	15.5	10.6	2403	34
B	6.4	4.0	15.3	73.7	15.4	13.8	2324	41
C	5.6	4.5	14.0	67.8	14.4	10.7	2389	40
D	6.0	5.1	13.1	61.3	18.6	11.1	2319	52
E	5.7	5.5	13.2	58.7	19.0	12.6	2327	47
F	6.4	5.9	15.1	61.6	22.0	12.7	2289	56
G	5.8	4.1	14.2	70.9	13.1	11.2	2350	72

AC = Asphalt Cement; VMA = Voids in Mineral Aggregate; VFA = Voids Filled with Asphalt

Table 7: Summary of Regression Analysis on Volumetric Properties

Mix Parameter	Correlation (R^2) to Rutting Rate	
	As-Constructed (Job Summary)	Present Condition (Recovered Cores)
Asphalt Cement Content	0.004	0.044
Air Voids	0.008	0.010
Voids in Mineral Aggregate	0.070	0.072
Marshall Stability	0.083	0.040
Recovered Binder Penetration	---	0.241
Density	0.044	0.033

5.2.2 Aggregate Properties

Aggregate gradation was determined for each of the recovered core samples. All gradations fell within acceptable limits specified by Manitoba Highways as summarized in Table 8. Sites E and G have the highest percentage of coarse aggregate at 36.7 and 38.2 percent, respectively. Site D has the highest percentage of fine aggregate at 65.7 percent while site F has the highest percentage of additive at 30.3 percent. Site F also has the highest amount of mineral filler at 6.5 percent.

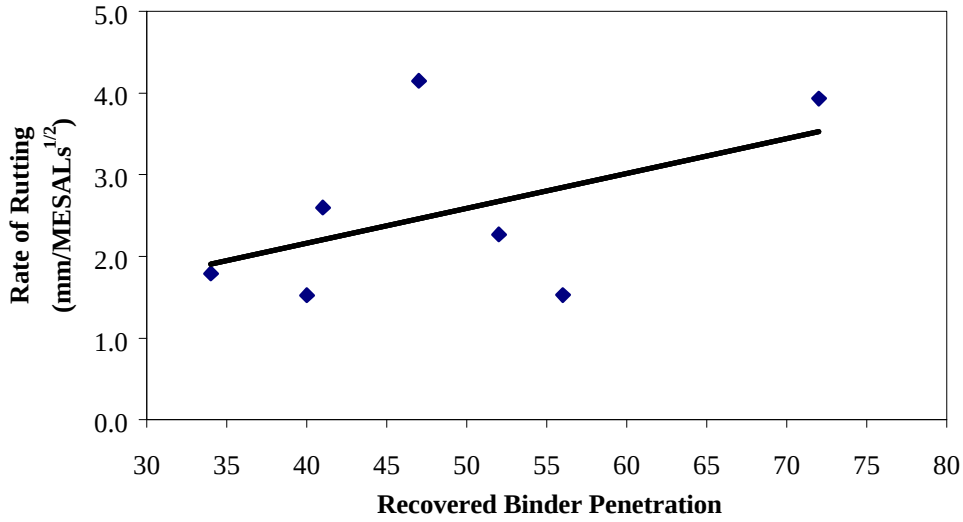

Figure 7: Recovered Binder Penetration vs. Rutting Performance

Table 8: Summary of Aggregate Properties

Test Site	Coarse Aggregate[1] (%)	Fine Aggregate[2] (%)	Mineral Filler[3] (%)
A	35.8	64.2	4.9
B	35.3	64.7	4.0
C	35.0	65.0	5.5
D	34.3	65.7	5.6
E	36.7	63.3	5.9
F	35.0	65.0	6.5
G	38.2	61.8	4.6

Note: [1] All material retained on the 4.75 mm (No. 4) sieve
[2] All material passing the 4.75 mm (No. 4) sieve
[3] All material passing the 75 µm (No. 200) sieve. The percent of mineral filler is included in the percent of fine aggregates

5.3 Results of Strength Testing

The load-deformation response of each sample was analysed and the ultimate load and corresponding failure strains determined. The tensile strength, S_T, of each sample was then calculated according to ASTM D 4123 [1]:

$$S_T = \frac{2 P_{ult}}{p \ t D}$$

where

P_{ult} = ultimate applied load, N
t = thickness of specimen, mm
D = diameter of specimen, mm

The test results are summarized in Table 9. Tensile strengths range from 30.7 to 138.3 kPa with an average of 90.6 kPa. These strengths are considerably lower than those reported by Kennedy [13] who suggested a tensile strength range of 172 to 3966 kPa for asphalt concrete depending on the test temperature. The discrepancy is a result of using a slower rate of loading in this study.

Site E exhibited the highest tensile strength (average S_T = 134.6 kPa) although it also had the highest rate of rutting. The lowest tensile strength was found for site G (average S_T = 31.4 kPa), which had the second highest rate of rutting behind site E. One possible explanation for this phenomenon is that some of the rutting at site E could be related to the underlying structure and not the asphalt layer only as was assumed.

The measured horizontal failure strains are consistently higher than the corresponding vertical values. The average horizontal and vertical strain values are 12,237 and -10,298 microstrains, respectively. Relatively good repeatability was observed at all sites except site B where the horizontal and vertical strains at failure for sample 1 were roughly twice those measure for sample 2. Nothing observed during the testing process could explain this result.

Table 9: Summary of Modified Indirect Tensile Strength Testing

Test Site	Sample	Ultimate Load, P_{ult} (N)	Tensile Strength, S_T (kPa)	Average Tensile Strength, S_T (kPa)	Strain at P_{ult} (microstrain) Horizontal (Lateral)	Vertical (Axial)
A	1	951.9	104.1	99.1	12,193	-10,484
	2	889.8	94.1		10,998	-11,876
B	1	660.0	78.0	81.8	20,578	-17,954
	2	733.9	85.6		10,559	-8,842
C	1	650.9	91.9	83.5	13,122	-8,667
	2	466.8	75.2		13,549	-12,212
D	1	883.1	109.4	107.2	14,829	-12,230
	2	872.4	105.1		11,953	-10,385
E	1	1090.8	138.3	134.6	9,893	---*
	2	1060.7	130.9		9,128	-5,570
F	1	1010.0	99.0	96.4	10,037	-9,074
	2	925.7	93.9		12,460	-12,791
G	1	283.8	30.7	31.4	9,178	-6,497
	2	272.0	32.0		12,837	-8,761

* No value obtained due to problems with a vertical LVDT.

Procedures developed by Buttlar and Roque [24] were utilized to determine stresses and strains at the centre of the samples during loading. Stress-strain response curves for all samples are shown in Figure 8. Deformations at 25 percent of the peak load were used to calculate stress and strain. The stress-strain response between samples showed very good correlation, particularly prior to peak loads. Cracking and disintegration of the samples caused the discrepancy in the results after the peak load. The peak load and rate of strain mobilization were consistent in most cases.

Sites D, F, and G show remarkable consistency between samples with regards to both the magnitude and rate of strain mobilization while sites A and C show good consistency with regards to the rate of strain mobilization only. Samples tested for sites B and E, however, show some disagreement in both areas.

This could be attributed to variability in the mix at the time of construction, resulting in cores with different material properties although taken from the same site.

A summary of the measured strain ratio and the calculated Poisson's ratio is shown in Table 10. Poisson's ratio was calculated according to the method outlined by Buttlar and Roque [24] using average deformations from both tested samples. The deformations used to calculate Poisson's ratio, however, were taken at 10 and 25 percent of the average failure load, P_{ult}, compared with 50 percent as specified, to account for the smaller loading rate. There does not appear to be a significant difference between the strain ratio or Poisson's ratio at 10 and 25 percent of the ultimate failure load, although the ratios tend to decrease from 10 to 25 percent. The highest strain ratios were measured on the samples of sites E (0.98 and 0.86 at 10 and 25 percent, respectively) and G (1.25 and 0.98 at 10 and 25 percent, respectively). These two sites also had the highest overall rate of rutting as discussed earlier. The remaining sites had strain ratios ranging from 0.37 to 0.81.

Similarly, the highest calculated values of Poisson's ratios were found for sites E and G. Site E had Poisson's ratios of 1.25 at 10 percent and 0.97 at 25 percent, while site G had Poisson's ratios of 1.69 at 10 percent and 0.95 at 25 percent of the ultimate load. These values indicate plastic flow of the material under the slow loading rate. It must be noted that although Poisson's ratio is thought to be valid only in the range of 0.05 to 0.5 [20], higher values were calculated here and have been left as such for this study.

The initial tangent modulus was obtained as a derivative of a fitted third order polynomial to the stress-strain curve at a strain of zero. The initial tangent modulus provides a suitable measure of short-loading-time stiffness [24]. The results are also shown in Table 10 and range from 9.5 to 66.7.

Table 10: Lateral to Axial Strain Ratio, Poisson's Ratio, and Initial Tangent Modulus

Test Site	Sample	Strain Ratio at 10% P_{ult}	Strain Ratio at 25% P_{ult}	Poisson's Ratio, ν, at 10% P_{ult}	Poisson's Ratio, ν, at 25% P_{ult}	Initial Tangent Modulus at 25% of P_{ult} (MPa)
A	1	0.81	0.77	0.52	0.50	27.6
	2	0.56	0.55			30.7
B	1	0.71	0.65	0.33	0.51	16.4
	2	0.37	0.66			30.5
C	1	0.65	0.70	0.37	0.42	22.5
	2	0.53	0.54			17.7
D	1	0.65	0.68	0.55	0.57	31.3
	2	0.71	0.68			34.4
E	1	---*	---*	1.25**	0.97**	54.4
	2	0.98	0.86			66.7
F	1	0.61	0.53	0.33	0.29	34.3
	2	0.52	0.52			31.0
G	1	0.77	0.62	1.69	0.95	14.9
	2	1.25	0.98			9.5

P_{ult} = ultimate applied load (N)

* No value obtained due to problems with a vertical LVDT

** Only one sample used to determine Poisson's ratio due to problems with a vertical LVDT during one of the tests

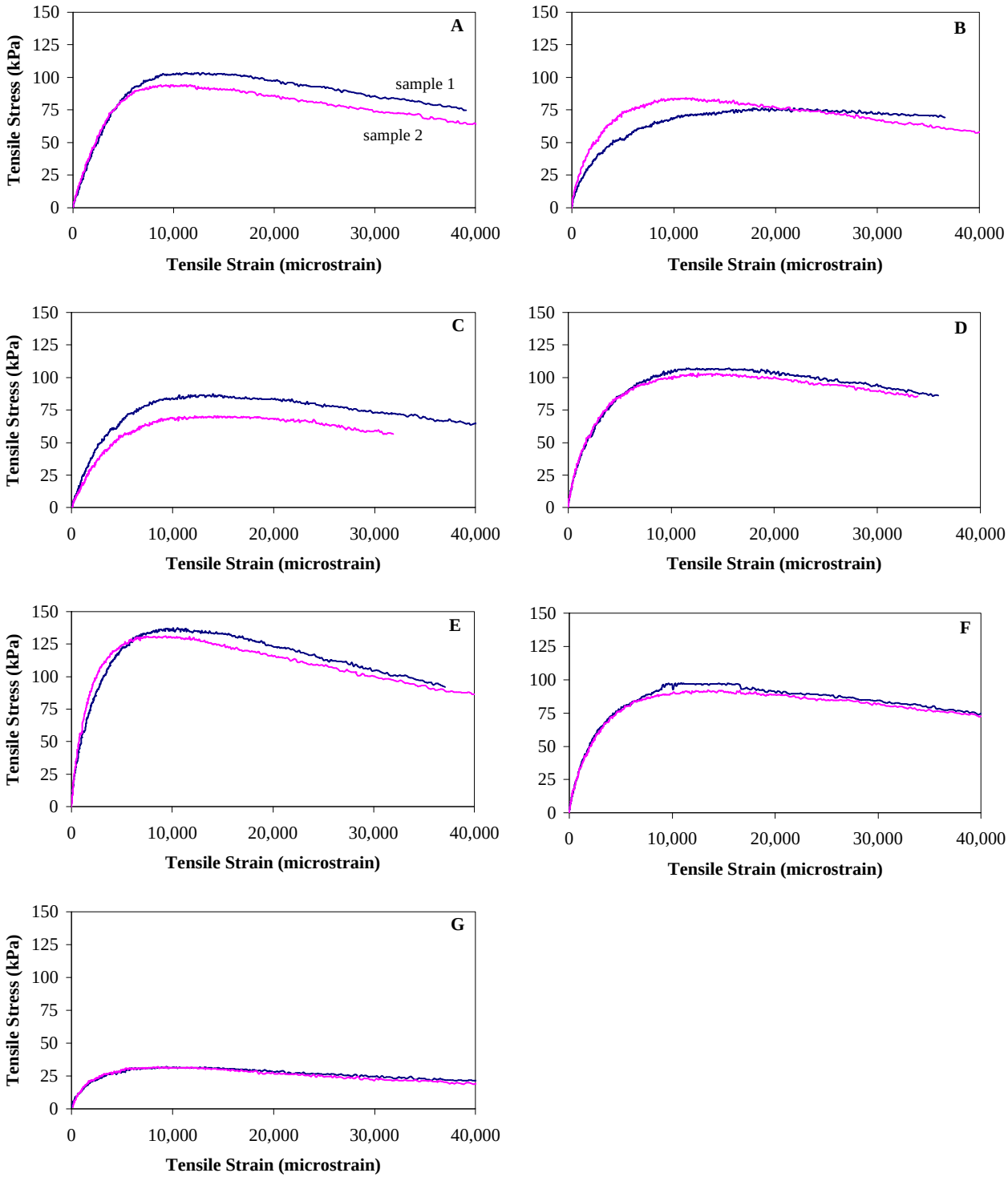

Figure 8: Stress-strain Response from Indirect Tensile Testing
(Strains are averaged from the two sample faces, two replicate samples per project)

5.4 Regression Analysis

Linear regression analysis of the test results shown in Tables 9 and 10 was performed to identify properties that correlate to the rate of rutting. As shown in Figure 9, the tensile strength of the asphalt mixtures showed no correlation with rate of rutting with an R^2 of only 0.011. This finding compares favourably with work done by Brown and Cross [21], who found little correlation between indirect tensile strength and rutting as a percentage of layer thickness. This is not surprising because rutting is generally associated with shear response to a sustained load rather than to tensile strength. Measured horizontal (tensile) strains at failure also show little correlation (R^2 = 0.084) with rate of rutting as presented in Figure 10.

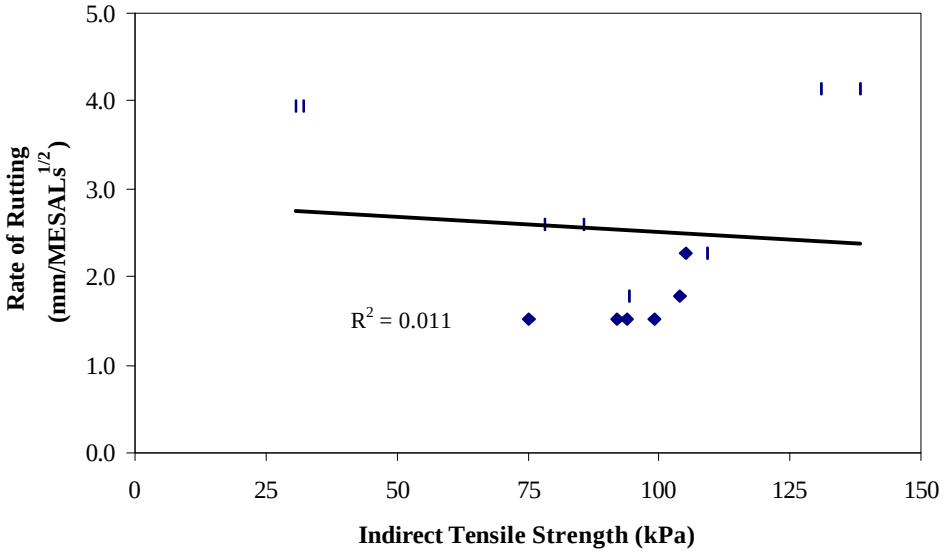

Figure 9: Indirect Tensile Strength vs. Rate of Rutting

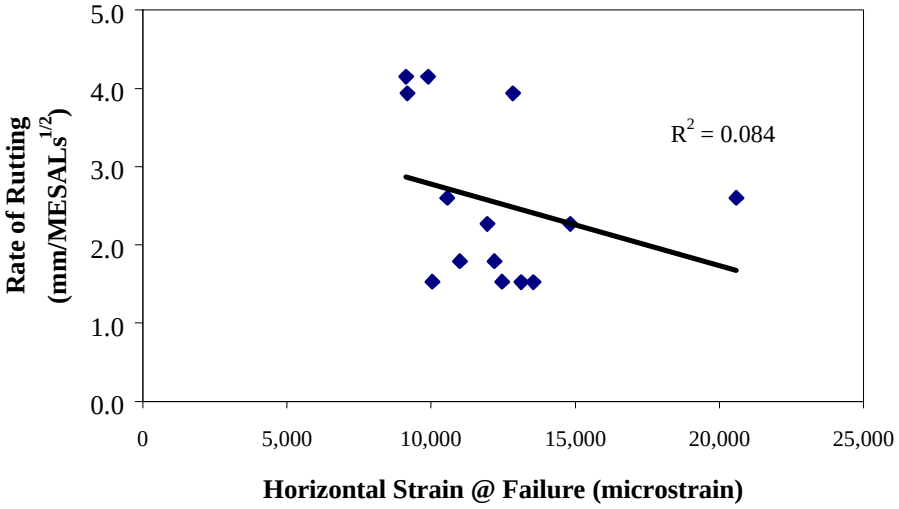

Figure 10: Measured Horizontal Strain at Failure vs. Rate of Rutting

Figure 11 shows the relationship between initial tangent modulus and rate of rutting. No correlation was found between the two with an R^2 of only 0.089.

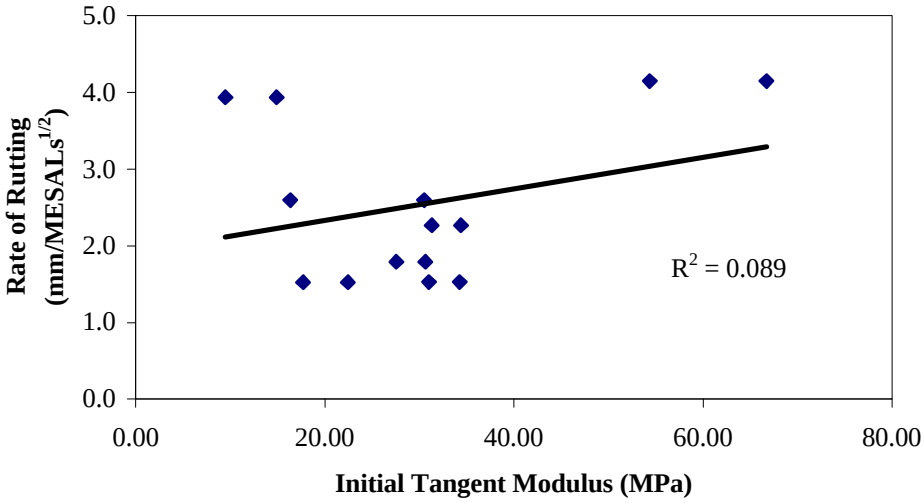

Figure 11: Initial Tangent Modulus vs. Rate of Rutting

Because rutting is associated with shear deformations, it is reasonable to expect that the ratio of lateral to axial strains in the indirect tensile test mode should correlate to the rate of rutting. Figure 12 shows the relationship between the ratio of measured horizontal (lateral) and vertical (axial) strain to the rate of rutting for measurements taken at 10 and 25 percent of the peak load. A better correlation is observed for both 10 and 25 percent with R^2 values of 0.479 and 0.452 respectively. In both cases, as the strain ratio increases the expected rate of rutting also increases.

A similar relationship between calculated values of Poisson's ratio and the rutting rate was also found. Figure 13 shows the relationship between the Poisson's ratio and rutting rate using deformation values at 10 and 25 percent of the peak load. An excellent correlation is observed in both cases with R^2 values of 0.791 and 0.935, respectively. It should be noted that Poisson's ratio is calculated as the average of each two replicate specimens. These results suggest that a testing protocol that measures the lateral and axial deformations of asphalt concrete mixes at monotonic or creep loads can produce reasonable predictions of rutting behaviour. These observations should be viewed in the context of the limited number of tested samples and the scope of this study.

6.0 CONCLUSIONS AND RECOMMENDATIONS

Previous research has shown that rutting performance can be correlated to strength and deformation properties. In this research, using a limited data set from test sections in Manitoba, a testing program covering strength and volumetric properties was carried out. The test sections were selected to represent various material and loading conditions in the province. Strength testing was performed using a modified indirect tensile strength test at a loading rate of 0.1 mm/min and at a temperature of 25°C. The loading rate was arbitrarily selected to be much lower than typical indirect tensile strength tests and the temperature was set to represent the dominant warm temperature conditions in Manitoba with a mean high 7-day air temperature of 30°C.

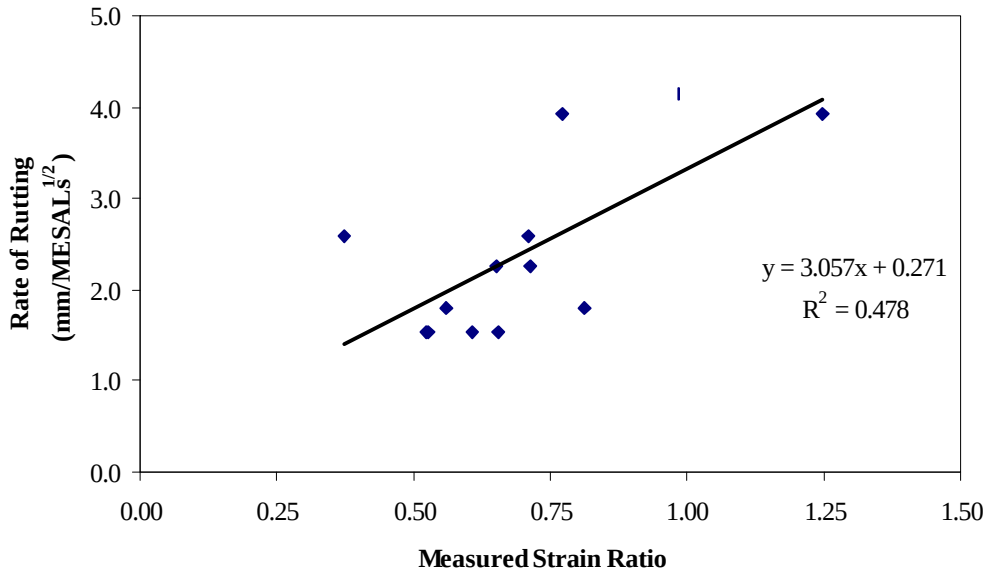

a) At 10 Percent of the Peak Load

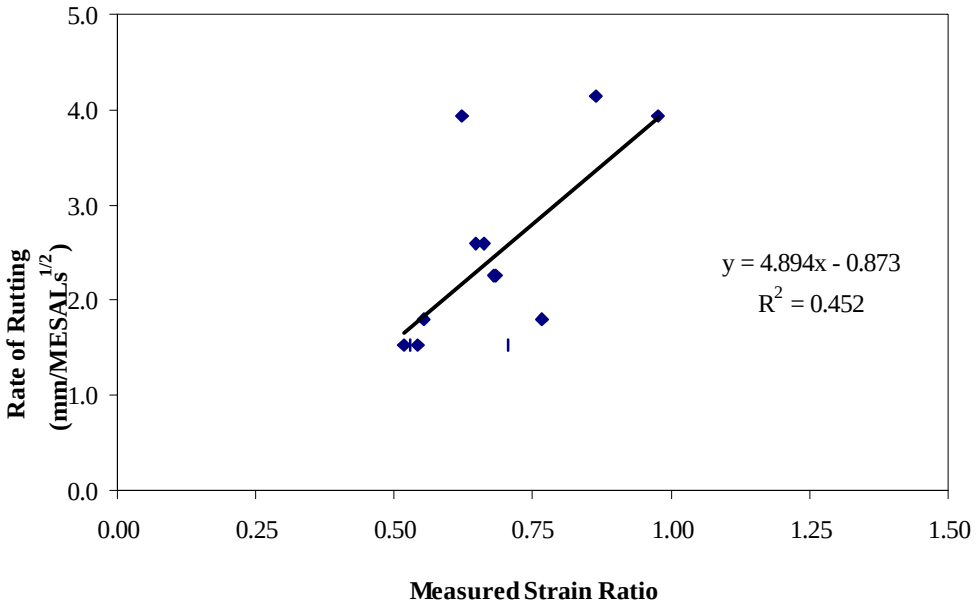

b) At 25 Percent of the Peak Load

Figure 12: On-sample Lateral to Axial Strain Ratio vs. Rate of Rutting

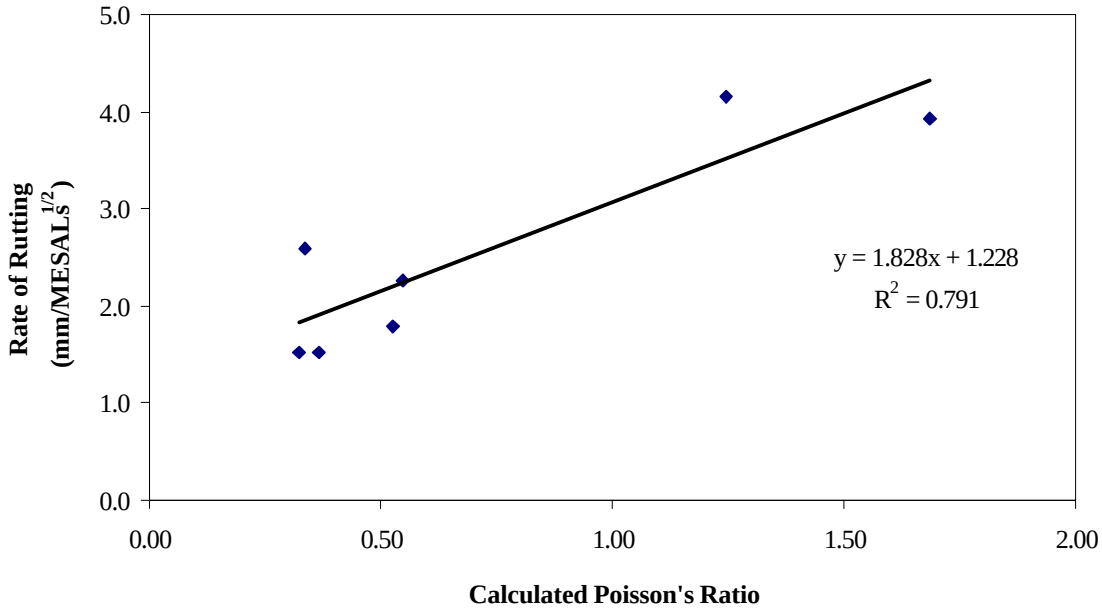

a) At 10 Percent of the Peak Load

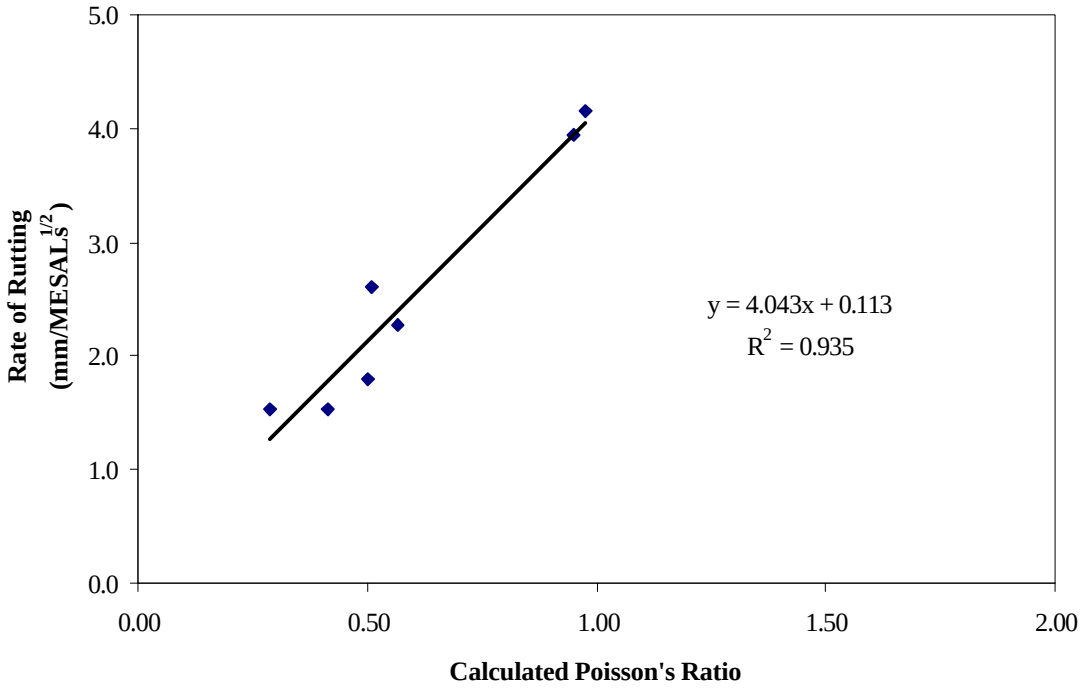

b) At 25 Percent of the Peak Load

Figure 13: Calculated Poisson's Ratio vs. Rate of Rutting
(average of two replicate samples)

The paper attempted to explore correlations between the rate of rutting as a performance indicator and several mix volumetric and strength properties. Since asphalt mixtures tend to exhibit higher rates of deformation in the early stages of traffic compaction, the rate of rutting is adjusted to be proportional to the square root of traffic in accumulated million ESALs. The focus of this research has been to investigate rutting caused by the instability of asphalt mixes, and hence only thick and overlaid pavements were included. It was, however, not possible to quantify the amount of structural rutting that took place, if any. Strength testing was performed on samples extracted from areas between the wheel paths, which are less exposed to traffic-induced damage. The testing supported the following observations:

1. Of the volumetric properties that were examined, the recovered binder penetration showed the strongest correlation to performance.
2. From the strength testing, it appears that peak (ultimate) stresses or strains do not correlate to rutting. Tensile strength (S_T) and values of strain at failure did not provide a correlation to rutting performance.
3. Poisson's ratio or a lateral to axial strain ratio taken at 10% or 25% of the ultimate load were found to be highly proportional to the rutting rate.
4. Although within the domain of elastic behaviour Poisson's ratio must not exceed 0.5, it was found that in some samples a significant flow occurred at a load level of 10 percent of the ultimate load. The flow resulted in horizontal deformation or cracking leading the calculated Poisson's ratio to exceed 0.5.
5. At this stage, the stress-strain response of replicate samples proves that the test is repeatable, in particular up to 25% of peak loads.
6. The measured strain ratio and Poisson's ratio obtained from a modified indirect tensile strength test shows promise as a means to evaluate mixture strength and relate laboratory test results to rate of rutting.

The following recommendations are made based on this study:

1. The modified indirect tensile strength test procedure as outlined in this paper can be used to evaluate asphalt concrete mix designs. The test set-up is relatively simple and cost effective, and test results are repeatable.
2. Additional testing should be conducted to verify the observations made in this study and to analyze the effect of changing the test temperature or loading rate.

7.0 REFERENCES

1. American Society for Testing and Materials. "ASTM D 4123-82(95): Standard Test Method for Indirect Tension Test for Resilient Modulus of Bituminous Mixtures" Annual Book of ASTM Standards, Vol. 04.03, American Society for Testing and Materials, Philadelphia; 423-425 (1995).
2. Federal Highway Administration. "Wanted: A Simple Superpave Performance Test" FOCUS, U.S. Department of Transportation, Federal Highway Administration, May (2000).
3. Finn FN, Monismith CL, Markevich NJ. "Pavement Performance and Asphalt Concrete Mix Design" Proceedings, Association of Asphalt Paving Technologists 52 121-144 (1983).
4. Monismith CL, Tayebali AA. "Permanent Deformation (Rutting) Considerations in Asphalt Concrete Pavement Sections" Proceedings, Association of Asphalt Paving Technologists 57 414-441 (1988).

5. Krutz NC, Stroup-Gardiner M. "Relationship Between Permanent Deformation of Asphalt Concrete and Moisture Sensitivity" Transportation Research Record No. 1259, 169-177 (1990).

6. Kim JR, Drescher A, Newcomb DE. "Rational Test Methods for Predicting Permanent Deformation in Asphalt Concrete Pavement" Report No. 93-08, Minnesota Department of Transportation (1991).

7. Kandhal PS, Cross SA, Brown ER. "Heavy-Duty Asphalt Pavements in Pennsylvania: Evaluation for Rutting" Transportation Research Record No. 1384, 49-58 (1993).

8. Brown ER, Foo KY. "Comparison of Unconfined- and Confined-Creep Tests for Hot Mix Asphalt" Journal of Materials in Civil Engineering 6 (2) 307-326 (1994).

9. Brown SF, Gibb MJ. "Validation Experiments for Permanent Deformation Testing of Bituminous Mixtures" Proceedings, Association of Asphalt Paving Technologists 65 255-289 (1996).

10. Bhairampally RK, Lytton RL, Little DN. "A Numerical and Graphical Method to Assess Permanent Deformation Potential for Repeated Compressive Loading of Asphalt Mixtures" Proceedings, 79th Annual Meeting Transportation Research Board (1999).

11. Krutz NC, Sebaaly PE. "The Effects of Aggregate Gradation on Permanent Deformation of Asphalt Concrete" Journal, Association of Asphalt Paving Technologists 62 450-473 (1993).

12. Xicheng Q, Sebaaly PE, Epps JA. "Evaluation of Polymer-Modified Asphalt Concrete Mixtures" Journal of Materials in Civil Engineering 7 (2) 117-124 (1995).

13. Kennedy TW. "Characterization of Asphalt Pavement Materials Using the Indirect Tensile Test" Proceedings, Association of Asphalt Paving Technologists 46 132-150 (1977).

14. Button JW, Perdomo D, Lytton RL. "Influence of Aggregate on Rutting in Asphalt Concrete Pavements" Transportation Research Record No. 1259 141-152 (1990).

15. Al-Abdul Wahhab H, Khan Z. "A Laboratory Evaluation of Two Asphalt Mix Design Methods and Characterization Tests to Assess Rutting Potential" Australian Road Research 21 (4) 78-88 (1991).

16. Zhang W, Drescher A, Newcomb DE. "Viscoelastic Behavior of Asphalt Concrete in Diametral Compression" Journal of Transportation Engineering 123 (6) 495-503 (1997).

17. Sousa JB, Solaimanian M. "Abridged Procedure to Determine Permanent Deformation of Asphalt Concrete Pavements" Transportation Research Record No. 1448, 25-33 (1993).

18. Tayebali AA, Khosla NP, Malpass GA, Waller HF. "Evaluation of Superpave Repeated Shear at Constant Height Test to Predict Rutting Potential of Mixes: Performance of Three Pavement Sections in North Carolina" Transportation Research Record No. 1681, 97-105 (1999).

19. Kandhal PS, Mallick RB. "Evaluation of Asphalt Pavement Analyzer for HMA Mix Design" NCAT Report No. 99-4, National Center for Asphalt Technology (1999).

20. Federal Highway Administration. "LTPP Protocol P07: Test Method for Determining the Creep Compliance, Resilient Modulus and Strength of Asphalt Materials Using the Indirect Tensile Test Device" Version 1.0, U.S. Department of Transportation, Federal Highway Administration, April (2000).

21. Brown ER, Cross SA. "A Study of In-Place Rutting of Asphalt Pavements" Proceedings, Association of Asphalt Paving Technologists 58 1-31 (1989).

22. Bissada AF. “Compactibility of Asphalt Paving Mixtures and Relation to Permanent Deformation” Transportation Research Record No. 911, 1-10 (1983).

23. Huber GA, Heiman GH. “Effect of Asphalt Concrete Parameters on Rutting Performance: A Field Investigation” Proceedings, Association of Asphalt Paving Technologists 56 33-61 (1987).

24. Roque R, Buttlar W, Ruth BE, Dickison SW. “Short-loading-time Stiffness from Creep, Resilient Modulus, and Strength Tests using Superpave Indirect Tension Test” Transportation Research Record No. 1630, 10-20 (1998).